Research article

Lactobacillus plantarum Shinshu N-07 isolated from fermented *Brassica rapa* L. attenuates visceral fat accumulation induced by high-fat diet in mice

T. Yin[1,2], S. Bayanjargal[1,2], B. Fang[1], C. Inaba[3], M. Mutoh[4], T. Kawahara[3], S. Tanaka[3] and J. Watanabe[1,2,5*]

[1] Food Research Institute, National Agriculture and Food Research Organization, Tsukuba, 305-8642, Japan; [2] School of Integrative and Global Majors, University of Tsukuba, Tsukuba, 305-8577, Japan; [3] Academic Assembly (Institute of Agriculture), Shinshu University, Minamiminowa, 399-4598, Japan; [4] Epidemiology and Prevention Division, National Cancer Center, Tokyo, 104-0045, Japan; [5] Department of Food Science, Obihiro University of Agriculture and Veterinary Medicine, Obihiro, 080-8555, Japan; nabej@obihiro.ac.jp

Running header
Anti-adiposity effect of *L. plantarum* Shinshu N-07 in mice

Abstract

Lactobacillus plantarum Shinshu N-07 (N07) and *Lactobacillus curvatus* #4G2 (#4G2) were isolated from fermented *Brassica rapa* L. and selected as promising probiotics with anti-adiposity activities based on *in vitro* assays. The anti-adiposity effects of these two strains were investigated using a diet-induced obesity animal model. Epididymal adipose tissue weight and adipocyte area were significantly lower and serum triglycerides and glucose tended to be lower in mice fed the high-fat diet supplemented with N07 compared with those fed the unsupplemented high-fat diet. Strain N07 suppressed hepatic steatosis, with accompanying downregulation of lipogenic genes in the liver. Expression of inflammatory cytokines and macrophage infiltration markers tended to be suppressed by N07 supplementation. Upregulation of uncoupling protein-1 in epididymal adipose tissue by N07 suggested that the transformation of white adipose tissue to brown might have been induced. Intestinal microbiota analysis revealed that a decrease in abundance of family *S24-7* (phylum *Bacteroidetes*) following ingestion of the high-fat diet was partly recovered by supplementation with N07. Changes in those parameters were not observed in mice fed the high-fat diet supplemented with strain #4G2, suggesting strain specificities. Thus, N07 is a potential probiotic strain that could be used to develop functional foods that attenuate visceral fat accumulation after an appropriate human intervention trial.

Keywords: fermented *Brassica rapa* L., anti-adiposity effect, *Lactobacillus plantarum*, high-fat diet, intestinal microbiota

1. Introduction

Obesity is defined as abnormal lipid accumulation, and it is a major health concern in both developing and developed countries. The prevalence of obesity has increased more than two-fold in the last 30 years. Obesity is the result of a long-term imbalance of energy consumption and expenditure, and it is associated with visceral fat accumulation that induces a chronic state of low-grade inflammation and immune dysfunction (Sanz *et al.,* 2010; Wolowczuk *et al.,* 2008; Verwaerde *et al.,* 2006). Obesity reportedly

increases the risk of various metabolic diseases, such as cardiovascular diseases, hypertension, and type II diabetes (Cumbie *et al.,* 2008; Karnik *et al.,* 2007).

Brassica rapa L., also known as nozawana, is a traditional leafy vegetable in Japan. *B. rapa* L. is often consumed as a lactic acid-fermented pickle called nozawana-zuke in the Nagano area of Japan. We previously reported that *B. rapa* L. enhanced innate immunity via activation of natural killer cells (Yamamoto *et al.,* 2018), and that butyrate production was enhanced by ingestion of the plant, with resulting immune-modulating effects in mice (Tanaka *et al.,* 2016). *Lactobacillus curvatus* is the predominant species during the fermentation of *B. rapa* L., followed by *Lactobacillus plantarum* and *Lactobacillus brevis* (Sandagdorj *et al.,* 2019). These lactobacilli induce IFN-γ and IL-10 production in immune cells of mice (Sandagdorj *et al.,* 2019).

Probiotics are defined as viable microbial dietary supplements that have beneficial effects on the health of the host organism (Fuller, 1989). Probiotics survive the gastrointestinal environment and affect bacterial ecology and metabolic activities in the gut. A large part of probiotic bacteria are *Lactobacillus* and *Bifidobacterium* species. Some strains of probiotic *Lactobacillus* are reported to be effective against obesity and obesity-related metabolic syndromes as well as gastrointestinal disorders such as irritable bowel syndrome and immune disorders (Masood *et al.,* 2011; Parvez *et al*., 2006).

The physiological functions of probiotic bacteria depend mainly on the strain rather than on the species to which they belong. Many *in vitro* assay systems have been developed and used to screen promising probiotic strains. Bacterial bile salt hydrolase (BSH) cleaves the amino acid side chain of glyco- or tauro-conjugated bile acids to generate unconjugated bile acids, which are further converted to secondary bile acids, such as deoxycholic acid and lithocholic acid, by intestinal microbes (Begley *et al*., 2005). Because deconjugated bile salts are more readily excreted in feces than conjugated bile salts (De Smet *et al*., 1998), bacteria showing BSH activity, as well as those possessing cholesterol assimilation activities, may improve lipid metabolism and play profound role in body weight gain in the host (Huang *et al*., 2013; Joyce *et al*., 2014).

The mammalian gut is colonized by a diverse microbiota that is known to modulate energy metabolism of the host. The gut microbiota is associated with induction of obesity and obesity-associated disorders, such as hyperlipidemia, insulin resistance, and diabetes (Lee *et al*., 2019). Manipulation of the intestinal microbiota by administration of prebiotics (Hamilton *et al*., 2017) or probiotics (Kim *et al*., 2017; Park *et al*., 2017) has been shown to have a beneficial effect on adiposity, insulin sensitivity, and low-grade inflammation.

In this study, we screened promising probiotic strains exhibiting anti-adiposity effects from *Lactobacillus* strains isolated from fermented *B. rapa* L. Then, we evaluated their effects on visceral fat accumulation in mice fed a high-fat diet. To clarify the mechanisms involved, we compared the intestinal microbiota and gene expression in adipose tissue and liver among mice fed a high-fat diet and those fed a high-fat diet supplemented with one of two strains from fermented *B. rapa* L.

2. Materials and methods

Isolation of lactic acid bacteria from fermented *B. rapa L.*

Fermented *B. rapa* L. was prepared according to our previous method (Sandagdorj *et al*., 2019) or purchased from retail sources in Nozawa-onsen village, Nagano, Japan. Lactic acid bacteria (LAB) were isolated from fermented *B. rapa* L. according to the method described previously (Sandagdorj *et al*., 2019).

Bile salt and low pH resistance, cholesterol assimilation, and bile salt hydrolase tests of LAB isolates

Bile salt and low pH resistance tests were conducted according to the method of Guo et al (2011). Cholesterol assimilation of LAB isolates was evaluated according to the protocol of Tomaro-Duchesneau *et al*. (2015) using cholesterol PEG600 (Sigma, St. Louis, MO, USA). BSH activity was evaluated as described by Liong and Shah (2005) using 6 mM sodium taurocholate as a substrate.

16S rRNA gene sequencing

Genomic DNA was extracted from colonies on a de Man, Rogosa, Sharpe (MRS; BD Difco, Sparks, MD, USA) agar plate using a QIAamp DNA Stool Mini Kit (Qiagen, Hilden, Germany) and a ZircoPrep Mini Kit (Nippon Genetics, Tokyo, Japan) according to the manufacturers' instructions. DNA concentration was quantified, followed by PCR amplification of the 16S rRNA gene using 27f and 1492r as primers (Taguchi *et al*., 2008). The amplified fragment was cloned into pMD20 (TakaraBio, Otsu, Japan), and the construct was introduced into ECOS Competent *E. coli* DH5α cells (Nippon Gene, Tokyo, Japan) for sequencing. Primers 529r, 786f, 926r, T7W, and SP6W (Taguchi *et al*., 2008) were used for gene-sequencing reactions. The 16S rRNA gene sequence was compared with sequence data in a public database using the blastn program (https://blast.ncbi.nlm.nih.gov/Blast.cgi) of NCBI BLAST Search (Altschul *et al*., 1990).

Species-specific PCR

Bacterial genomic DNA was amplified by PCR with primer pairs (Table S1) specific for *L. brevis* (Fusco *et al*., 2016), *L. curvatus* (Berthier *et al*., 1999), or *L. plantarum* (Torriani *et al*., 2001). The PCR reaction mixture (25 μL) contained 1× KOD-FX Neo buffer, 0.4 mM of each dNTP, 100 pM each of forward and reverse primers, and 0.6 U of KOD-FX Neo (Toyobo, Osaka, Japan). The reaction conditions were 94 °C for 3 min, 30 cycles at 94 °C for 30 s, 54 °C for 10 s, and 72 °C for 30 s, followed by 72 °C for 5 min. The resulting PCR product was mixed with SYBR Green I nucleic acid gel stain (Takara Bio), and the mixture was electrophoresed on 1.5 % (w/v) agarose gel. Genomic DNA from type strains of *L. brevis* (JCM1059), *L. curvatus* (JCM1096), or *L. plantarum* (JCM1149) was used as positive controls for PCR.

Preparation of freeze-dried bacterial powder

L. curvatus #4G2 (#4G2) and *L. plantarum* Shinshu N-07 (N07) were cultured in MRS (BD Difco) broth at 30 °C for 24 h. The cells were collected by centrifugation (50,000 ×

g, 10 min), washed with sterilized saline, and suspended in 25 % (w/w) skimmed milk (Yotsuba Milk, Sapporo, Japan). The resulting cell suspension was snap frozen in liquid nitrogen and then freeze-dried. Viable cell numbers in the freeze-dried powder were quantified by counting colonies on MRS agar plates. Viable cell numbers in the freeze-dried powder were adjusted to 2×10^{11} cfu/g by the addition of skimmed milk.

Animals and diets

Five-week-old male C57BL/6J mice were purchased from Japan Charles River (Yokohama, Japan) and housed in standard plastic cages in a temperature-controlled room (23 ± 2 °C) with a dark period from 2000 to 0800 h. They were acclimated for 1 wk by feeding an AIN93M composition diet (Reeves *et al*., 1993). Mice weighing 20.6 ± 0.1 g were divided into 4 groups of 8 animals each. Each group of mice was fed either a normal-fat diet (NFD), a high-fat diet (HFD), or supplemented high-fat diets HFD-#4G2 or HFD-N07. The HFD-#4G2 and HFD-N07 diets were prepared by supplementing freeze-dried powder of #4G2 or N07 (1×10^{10} cfu/g) to HFD60 (60% energy from fat, Oriental Yeast, Tokyo, Japan). For the NFD and HFD diets, skimmed milk was added to AIN93M and HFD60 (50 mg/g), respectively, instead of bacterial powder. Mice were fed each diet ad libitum for 8 wk. Diets were changed every other day, and the HFD-#4G2 and HFD-N07 diets were freshly prepared by the addition of freeze-dried bacterial powder to HFD. Viable bacterial numbers in HFD-#4G2 and HFD-N07 diets were quantified by counting colonies on MRS agar plates, and were not significantly changed after the storage at 25 °C for 2 d. At the end of the experimental period, mice were fasted for 12 h, anaesthetized with inhalation of isoflurane, and exsanguinated by cardiac puncture. The liver and epididymal adipose tissues were excised and weighed. Parts of each tissue were soaked in RNAlater (Qiagen, Valencia, CA, USA), and stored at −80 °C until use. Cecal contents were snap frozen in liquid nitrogen for microbiota analysis.

This animal experiment was approved by the Animal Use Committee of Food Research Institute, National Agriculture and Food Research Organization, and all mice were maintained in accordance with the guidelines for the care and use of laboratory animals of the research organization (approval no. H29-013).

Serum and liver biochemical analyses

Serum triacylglycerol (TG), total cholesterol (TC), and glucose were measured using commercial enzyme kits (Wako Pure Chemicals, Osaka, Japan). Approximately 300 mg of liver was freeze-dried, and total lipid was extracted with mixed solvent of chloroform and methanol (2:1). The extraction was repeated 3 times, and the solvent was evaporated under nitrogen gas flow. Total lipid was weighed and then dissolved in 10% (v/v) Triton X-100 in 2-propanol. Levels of TG and TC in the extract were measured using commercial kits (Wako Pure Chemicals).

Histology of epididymal adipose tissue and liver

Epididymal adipose tissue and liver were fixed in Mildform 10N (Wako Pure Chemicals) and embedded in paraffin. The sections (3 μm) were stained with hematoxylin-eosin. Images were taken under a microscope (BZ-8000; Keyence, Osaka, Japan) at a magnification of 200×, and adipocyte area was analyzed using Image J software (National Institutes of Health, Bethesda, MD, USA).

Reverse transcription-PCR

Total RNA was extracted from the liver and epididymal adipose tissue using TRIzol reagent (Thermo Fisher Scientific, Tokyo, Japan), and then purified with an RNA mini kit (Qiagen) according to the manufacturers' instructions. Reverse-transcription was performed using SuperScript III and an oligo $(dT)_{20}$ primer (Thermo Fisher Scientific). The cDNA was used for quantitative PCR using a KAPA SYBR Fast qPCR Master Mix (KAPA Biosystems, Wilmington, MA, USA). The relative quantification of expression levels was calculated by $^{\Delta\Delta}$Ct method with normalization to ribosomal protein S18 (Ogita *et al*., 2011). Primer sequences for reverse transcription (RT)-PCR analyses are shown in Table S2.

Microbiota analysis

DNA was extracted from cecal content and purified using a ZircoPrep Mini Kit (Nippon Genetics) and a QIAamp DNA Stool Mini Kit (Qiagen). DNA samples were quantified, followed by PCR amplification of the V3 and V4 regions of 16S rRNA genes with using 341F (5′-CCTACGGGNGGCWGCAG-3′) (Klindworth *et al*., 2013) and 806R (5′-GGACTACHVGGGTWTCTAAT-3′) (Kennedy *et al*., 2016) primers joined to the Illumina overhang adapter sequences. A second PCR was done to add barcodes to each sample. After quantification, amplicons were pooled in equal amounts, and pair-end 2 × 300 bp sequencing was performed using a MiSeq System (Illumina Inc., San Diego, CA, USA) and MiSeq Reagent Kit v3 (Illumina Inc.).

Sequences in demultiplexed format were analyzed using QIIME2 2019.4.0 (https://qiime2.org). Denoising of merged paired-end reads was done using DADA2 (Callahan *et al*., 2016). Sequence variants assigned as originating from chloroplast and mitochondria were eliminated from further analyses. For each representative sequence, the GreenGene database (McDonald *et al*., 2012) was used to annotate the taxonomic information (DeSantis *et al*., 2006). Alpha- and beta-diversities were analyzed by rarefying the feature table at a consistent sample depth of 13,500. To identify the representative taxa of each group, the linear discriminant analysis effective size (LEfSe) algorithm was then performed (Segata *et al*., 2011). Representative sequences of the most dominant sequence variants were compared with sequence data in a public database using the blastn program of NCBI BLAST Search (Altschul *et al*., 1990).

Statistical analyses

All data are presented as mean ± SEM. To compare mean values among all groups of mice, one-way ANOVA followed by the Tukey-Kramer post hoc test was applied. The Dunnett post hoc test was applied to compare the mean values of LAB-supplemented HFD-fed groups and those of the unsupplemented HFD control group. Bartlett's test for homogeneity of variances was performed to determine whether the variances were equal. Statistically significant outliers were removed after Smirnov-Grubbs test. All statistical analyses were conducted with a significance level of $P < 0.05$ using R ver. 3.5.1.

3. Results

Screening and identification of *Lactobacillus* strains from fermented *B. rapa L.*

Twenty LAB strains were isolated from fermented *B. rapa* L., and PCR using species-specific primers suggested that 2 strains were *L. brevis*, 4 were *L. curvatus*, and 14 were *L. plantarum* (Table 1). Of these 20 isolates, all were resistant to bile acid, and 18 showed survivability at pH 2.5 for 2 h. Of the 18 strains that tolerated low pH, 4 showed cholesterol assimilation. Of these, strains N07 and #4G2 showed the highest BSH activities among the isolates assigned as *L. plantarum* and *L. curvatus*, respectively. Thus, these two isolates were used for further *in vivo* experiments. Sequences of 16S rRNA genes of the strains N07 and #4G2 were deposited at DDBJ (http://getentry.ddbj.nig.ac.jp/top-e.html) under accession numbers LC494014 and LC201480, respectively.

Change in body and organ weights

Increases in body weight over time and weights of liver and epididymal adipose tissues of mice at 8 weeks are shown in Figure 1. All HFD-fed groups showed significantly increased body weight from 5 days after starting the experimental feeding compared with mice in the group fed NFD (Figure 1A). In addition, epididymal adipose tissue weight was significantly higher in all HFD-fed groups compared with the NFD group (Figure 1C). These results suggested that obesity was successfully induced by feeding of HFD. Among the HFD-fed groups, body weight gain was not significantly different among the groups. No significant differences were observed in liver weight among all experimental groups (Figure 1B). In contrast, weight of epididymal adipose tissue of HFD-fed groups was significantly greater than that of the NFD-fed group; it was significantly less in the HFD-N07 group, but not in the HFD-#4G2 group, compared with the HFD group (Figure 1C). Average diet consumption was not significantly different among the HFD-fed groups (data not shown). Calculated average LAB consumption of HFD-#4G2 and HFD-N07 groups was 2.3×10^{10} and 2.3×10^{10} CFU/day/mouse, respectively.

Serum parameters

Serum TG level of HFD-fed groups was significantly higher than that of the NFD-fed group (Figure 2A). Serum total TC level of HFD-fed groups tended to be higher than that of the NFD-fed group (Figure 2B). Serum glucose levels of mice in the NFD group tended to be higher than that of the HFD-fed groups (Figure 2C). Mice fed HFD-N07 tended to show decreased TC and glucose levels compared with those fed HFD, although such decreasing trends were not observed in the mice fed HFD-#4G2 (Figure 2B and 2C).

Lipid accumulation in the liver

Total lipid, TG, and TC in the liver were significantly higher in HFD-fed groups than in the NFD-fed group (Figure 3A, 3B, and 3C). Histological observation of liver confirmed induction of adiposity in the liver of mice fed HFD (data not shown). Among the HFD-fed groups, total lipid levels were significantly lower in the HFD-N07 group than in the unsupplemented HFD group (Figure 3A). Mice fed HFD-N07 tended to have decreased TG levels compared with those fed HFD (Figure 3B), although TC was not significantly different among the groups of mice fed HFD. Decreasing trends in hepatic lipid parameters were not observed in mice fed HFD-#4G2.

Microscopic evaluation of epididymal adipose tissue

The cross-sectional area of adipocytes in epididymal adipose tissue was significantly increased in HFD-fed groups compared with the NFD-fed group (Figure 4). Mice fed HFD-N07 had a significantly reduced cross-sectional area of adipocytes compared with those fed HFD (Figure 4E).

Gene expression in liver and adipose tissue

To explore the mechanisms by which LAB isolates from fermented *B. rapa* L. affect lipid metabolism in HFD-fed mice, we assessed expression of genes encoding proteins related to lipogenesis (*Acc1*, *Fas*), lipid β-oxidation (*Acox1*, *Cpt1*), and a regulator of

lipid metabolism (*Pparg*) in liver (Figure 5) and epididymal adipose tissue (Figure 6) by RT-PCR. Hepatic expression of *Acc1* in mice of the HFD-N07 group was significantly suppressed compared with that in the HFD group, although expression levels of *Fas* and genes involved in β-oxidation were unchanged by supplementation with LAB isolates (Figure 5). Hepatic *Pparg* expression was significantly suppressed in mice fed HFD-N07 compared with those fed HFD (Figure 5). Significant changes in the expression levels of these genes were not observed in the liver of mice fed HFD-#4G2 (Figure 5). In contrast, expression levels of *Acc1*, *Fas*, *Acox1*, *Cpt1*, and *Pparg* in epididymal adipose tissue were unchanged in mice fed the HFD supplemented with either of the LAB isolates (Figure 6). Upregulated expression of *Ucp1*, which contributes energy expenditure via thermogenesis, was observed in mice fed HFD-N07 compared with those fed HFD (Figure 6). Inflammation and macrophage infiltration markers in epididymal adipose tissue were also assessed by RT-PCR. N07 treatment tended to suppress these parameters in epididymal adipose tissue compared with the HFD-fed group (Figure 7, *P*-values between N07 and HFD groups: *Tnfa*, $P = 0.125$; *Il1b*, $P = 0.127$; *Cd11c*, $P = 0.167$).

Intestinal microbiota

High-quality 16S rRNA gene sequences (n = 1,709,360) were analyzed (average of 53,418 ± 6,185 sequences per sample). After quality filtration, denoising, and elimination of chimeric sequences with DADA2 (Callahan *et al*., 2016), 648,573 sequences (average of 20,267 ± 2,631 sequences per sample) were valid. Sequence variants assigned as originating from chloroplast and mitochondria were eliminated, and 370 sequence variants were obtained.

Mice in the HFD-N07 group had lesser alpha diversity than those in other groups, based on observed operational taxonomic units (OTUs) and Faith's phylogenetic diversity (Figure 8A and 8B). Although a clear separation of intestinal microbiota communities was observed between the mice fed NFD and those fed HFD in the principal coordinate analysis (PCoA) plot of unweighted UniFrac matrix, alteration of the microbiota by ingestion of LAB isolates was not obvious among mice in the HFD-fed groups (Figure 8C). To identify the specific bacterial groups associated with administration of LAB

isolates, we applied LEfSe analysis (Segata *et al*., 2011), and relative abundances of species among the groups of mice were compared. LEfSe revealed the enrichment of a range of bacterial taxa, from the phylum to the species levels in mice fed NFD, HFD, HFD-#4G2, and HFD-N07 (Figure S1). Among the bacterial groups which showed linear discriminant analysis (LDA) values of > 3, populations of bacterial groups assigned as o_*Lactobacillales*|f_|g_ (Figure 8D), f_*Lactobacillaceae*|_ (Figure 8E), and f_*S24-7*|g_ (Figure 8F) differed significantly with ingestion of N07 or #4G2. Representative sequences of the most dominant sequence variants classified as o_*Lactobacillales*|f_|g_ and f_*Lactobacillaceae*|_ showed the highest similarities with 16S rRNA sequences of *L. curvatus* and *L. plantarum*, respectively, and those were enriched in HFD-#4G2 or HFD-N07 groups. The population of f_*S24-7*|g_ was drastically decreased in mice fed HFD compared with those fed NFD, and supplementation of N07 partly recovered the decrease observed for this bacterial group.

4. Discussion

A large number of studies have focused on developing anti-obesity probiotics as food ingredients (Miyoshi *et al*., 2014). A meta-analysis on the effects of probiotics on control of body weight suggested that administration of *L. plantarum* and *Lactobacillus gasseri* was associated with body weight loss in obese humans and animals (Million *et al*., 2012). *L. plantarum* is preferentially found in fermented vegetables and fruits (Wouters *et al*., 2013; Di Cagno *et al*., 2013). We showed previously that *L. plantarum* and *L. curvatus* were the main contributors to fermentation of *B. rapa* L., which is traditionally produced and consumed in the Nagano area of Japan, and *Lactobacillus* isolates possessing immune-modulation activities have been isolated from fermented *B. rapa* L. (Sandagdorj *et al*., 2019). In the present study, we selected *L. curvatus* #4G2 and *L. plantarum* Shinshu N-07 based on *in vitro* assays, and evaluated their effects on body weight gain and visceral fat accumulation in an animal model of HFD-induced obesity. The rodent HFD model has been widely used to study visceral obesity because the pathogenesis of obesity in the model is similar to that in humans (Liao *et al*., 2013). In the current study, we demonstrated that mice fed HFD showed remarkable increases in body weight (Figure 1A), adiposity (Figure 1B and 1C), and enlargement of adipocytes in epididymal adipose tissue (Figure 4) compared with those fed NFD,

whereas HFD supplemented with N07 significantly suppressed the increase in epididymal adipose tissue weight (Figure 1C), and decreased liver steatosis (Figure 3A) and the cross-sectional area of adipocytes (Figure 4E). Thus, we confirmed that the model used here induced adiposity by the ingestion of HFD and that supplementation with N07 improved the status. In addition, controlling appetite is not likely to contribute the anti-adiposity effect of N07, because supplementation of N07 to HFD did not affect the average diet consumption.

It is widely recognized that most effects of probiotics are specifically observed in certain strains. Various *in vitro* screening systems have been used to screen probiotic strains with promising anti-adiposity effects, including measurements of BSH activity, cholesterol assimilation activity, and inhibition of lipid accumulation in 3T3-L1 cells (Liong *et al*., 2005; Tomaro-Duchesneau *et al*., 2015; Lee *et al*., 2018). In this study, we measured BSH and cholesterol assimilation activities of isolates as these are directly related to the prevention and treatment of HFD-induced adiposity (Tomaro-Duchesneau *et al*., 2014). N07 and #4G2 showed both activities; in addition, both strains were resistant to a simulated gastrointestinal atmosphere (Table 1). Thus, isolates from fermented *B. rapa* L., especially N07 and #4G2, are good candidates for anti-adiposity probiotics.

Total lipid content in liver was significantly lower and TG in the liver tended to be lower in the mice fed HFD-N07 compared with those fed HFD (Figure 3A and 3B), suggesting that HFD-induced liver steatosis was improved by ingestion of N07. To explore the mechanisms by which LAB isolates from fermented *B. rapa* L. affect lipid metabolism in HFD-fed mice, we assessed expression of genes encoding proteins related to lipogenesis, lipid β-oxidation, and a regulator of lipid metabolism in liver and epididymal adipose tissue by RT-PCR. Expression of *Acc1*, a lipogenesis gene, was significantly lower in the liver of mice in the HFD-N07 group than in those of the HFD group (Figure 5). In addition, decreased expression of *Pparg* in liver was observed in mice fed HFD-N07 (Figure 5). In contrast, changes in the expression levels of β-oxidation-related genes (*Acox1* and *Cpt1*) were not observed in mice fed N07 (Figure 5). Increased PPAR-γ has been reported in steatotic livers (Wu *et al*., 2015), and ingestion of N07 downregulated *Pparg* in liver (Figure 5). Thus, decreased lipogenesis

is likely to be involved in the improvement of liver steatosis by N07, and PPAR-γ might be one of the regulators that explain this effect with N07. In contrast to altered gene expression in the liver, altered expression of lipogenesis- or β-oxidation-related genes were not observed in epididymal adipose tissue (Figure 6), although the tissue weight was significantly less in mice fed HFD-N07 than in those fed HFD (Figure 1B). White adipose tissue has been recognized as an energy-storing tissue; however, its ability to dissipate energy was recently reported (Orci *et al*., 2004). The transformation of white adipose tissue as an energy-expending tissue is recognized as 'browning', and upregulation of UCP-1 is the most important biomarker of browning (Orci *et al*., 2004). Increased expression of *Ucp1* was observed in epididymal adipose tissue of mice fed N07 (Figure 6), suggesting that N07 induced browning of white adipose tissue, with a resulting decrease in epididymal adipose tissue.

Obesity is characterized by chronic, low-grade inflammation, a process in which recruited macrophages play an important role by producing proinflammatory cytokines such as TNF-α and IL-6 (Wagner *et al*., 2015; Olefsky *et al*., 2010). It has been reported that obesity-associated low-grade inflammation impairs insulin signaling, with resulting induction of metabolic syndrome (Russo *et al*., 2018). Probiotic strains of LAB reportedly suppress not only diet-induced adiposity but also impaired insulin sensitivity, with accompanying downregulation of proinflammatory cytokines in the adipose tissue. N07 tended to suppress elevation of gene expression of proinflammatory cytokines (*Tnfa* and *Il1b*) and a marker for recruited macrophages (*Cd11c*, Figure 7) (Lim *et al*., 2016). In addition, mice fed HFD-N07 tended to show lower fasting blood glucose than those fed HFD (Figure 2C). These results suggest that ingestion of N07 might have suppressed induction of obesity-induced metabolic syndrome.

The gut microbiota is reportedly associated with induction of obesity and obesity-associated disorders (Lee *et al*., 2019), and manipulation of the intestinal microbiota by the administration of prebiotics (Hamilton *et al*., 2017) or probiotics (Kim *et al*., 2017; Park *et al*., 2017) has been shown to have a beneficial effect on adiposity, insulin sensitivity, and low-grade inflammation. We performed amplicon sequencing of fragments of 16S rRNA gene to clarify the effects of ingestion of *Lactobacillus* isolates on the composition of intestinal microbiota of mice. Concerning alpha-diversity

parameters, observed OTUs and Faith's phylogenetic diversity were significantly decreased in the mice fed HFD-N07 (Figure 8A and 8B), indicating that ingestion of N07 induced a less-diverse intestinal microbiota. Increased bacterial diversity is associated with a greater microbial ecosystem stability and an improved health status of the host (Chen *et al*., 2017; Konopka, 2009). However, resveratrol suppressed the obesity induced by the high-fat diet, accompanied by changes in the intestinal microbiota with decreased bacterial diversity (Campbell *et al*., 2019). We applied LEfSe analysis and compared relative abundances of species among the groups of mice to identify specific bacterial groups associated with administration of *Lactobacillus* isolates. Among the bacterial groups which showed LDA values of > 3, populations of bacterial groups assigned as o_*Lactobacillales*|f_|g_ and f_*Lactobacillaceae*|_ were significantly higher in HFD-#4G2 and HFD-N07 groups, respectively, and their populations were very low in other groups (Figure 8D and 8E). Representative sequences of the most dominant sequence variants classified as o_*Lactobacillales*|f_|g_ and f_*Lactobacillaceae*|_ showed the highest similarities with 16S rRNA sequences of *L. curvatus* and *L. plantarum*, respectively. These results suggest that *L. curvatus* and *L. plantarum* are rarely observed in the intestine of mice, and that their populations can be increased by dietary supplementation of *Lactobacillus* isolates. LEfSe analysis also revealed that the population of f_*S24-7*|g_ was drastically decreased in mice fed HFD compared with those fed NFD, and supplementation of N07 partly recovered this decrease (Figure 8F). Family *S24-7*, a member of phylum *Bacteroidetes*, is associated with improved gut function and metabolic health (Ormerod *et al*., 2016). For example, increased abundance of *S24-7* by supplementation of dietary fiber was strongly correlated with suppression of inflammatory markers in obese mice (Serino *et al*., 2012). The co-treatment of quercetin and resveratrol suppressed HFD-induced obesity by modulating the gut microbiota with an increase of *S24-7* (Zhao *et al*., 2017). Gut epithelia protect the invasion of intact bacterial cells including LAB, suggesting that N07 is not likely to directly affect metabolism of mice. Thus, changes in the composition of gut microbiota by supplementation of N07 could contribute, at least partly, to the anti-adiposity effects. It has been reported that *in vitro* cholesterol assimilating activity of probiotic strains was inconsistent with their *in vivo* activity (Madani *et al*., 2013). Indeed, only N07 suppressed visceral fat accumulation *in vivo*, but both N07 and #4G2 had BSH and cholesterol assimilation activities. The HFD-

induced decrease in *S24-7* was partly recovered by N07 but not by #4G2 (Figure 8F). Although the reasons for differences in *in vivo* characteristics between the strains are unclear, this strain specificity might be caused by differences in the effects on intestinal microbiota between strains.

5. Conclusions

Twenty LAB strains were isolated from fermented *B. rapa* L. Among the isolates resistant to bile acid and low pH, N07 and #4G2 showed high cholesterol assimilation and BSH activities. Thus, we evaluated the anti-adiposity effects of these two isolates using an HFD-induced obesity model. Ingestion of HFD (60% energy from fat) induced obesity in C57BL/6J mice. Increases in epididymal adipose tissue and hepatic steatosis were suppressed by supplementation with N07. Suppression of lipogenesis in the liver might have contributed to the anti-adiposity effect of N07. Low-grade inflammation in adipose tissue, which is reportedly caused by obesity, tended to be suppressed by ingestion of N07. Although an altered composition of the intestinal microbiota was observed following ingestion of N07, the contribution of the intestinal microbiota to the anti-obesity effect of N07 remains unclear. Strain #4G2 failed to show an anti-adiposity effect in mice, despite its positive parameters in *in vitro* tests. Overall, our results indicate that N07 is a potential probiotic strain exhibiting an anti-adiposity effect.

Supplemental material

Table S1. Primer sequences for *Lactobacillus* species-specific PCR.
Table S2. Primer sequences for reverse transcription-PCR.
Figure S1. Cladogram for differentially abundant gut microbiota of mice fed a normal-fat diet, high-fat diet (HFD), HFD supplemented with *Lactobacillus curvatus* #4G2, and HFD supplemented with *Lactobacillus plantarum* Shinshu N-07 were constructed based on LEfSe analysis.

Acknowledgements

This work was supported by a grant from the program ‘Research Development for Discovering of Regional Agricultural Products and Foods having a Beneficial Impact on Health’ of the Ministry of Agriculture, Fishery and Forestry, Japan, and by JSPS KAKENHI Grant Number 18K11039. The amplicon analysis of the 16S rRNA gene was supported by the Advanced Genomics Breeding Section of Institute of Crop Science, NARO (NICS) (Project ID: 18A17). We would like to express our appreciation to Ms. Y. Toyama for technical support. We thank Louise Adam, ELS(D), from Edanz Group (www.edanzediting.com/ac) for editing a draft of this manuscript.

Figure legends

Figure 1. Body weight (A, from weeks 0 to 8), liver (B), and epididymal adipose tissue (C) weight (at 8 weeks) of mice fed a normal-fat diet (NFD), high-fat diet (HFD), and HFD supplemented with *Lactobacillus curvatus* #4G2 (#4G2) or *Lactobacillus plantarum* Shinshu N-07 (N07). Values are expressed as means ± SEM (n=8). **P* < 0.05 compared with the HFD group (Dunnett post hoc test).

Figure 2. Serum triglyceride (TG; A), total cholesterol (TC; B) and glucose (C) of mice fed a normal-fat diet (NFD), high-fat diet (HFD), and HFD supplemented with *Lactobacillus curvatus* #4G2 (#4G2) or *Lactobacillus plantarum* Shinshu N-07 (N07). Values are expressed as means ± SEM (n = 8). *P*-values between HFD and N07 groups of Dunnett post hoc test are shown.

Figure 3. Liver total lipid (A), triglyceride (TG; B) and total cholesterol (TC; C) of mice fed a normal-fat diet (NFD), high-fat diet (HFD), and HFD supplemented with *Lactobacillus curvatus* #4G2 (#4G2) or *Lactobacillus plantarum* Shinshu N-07 (N07). Values are expressed as means ± SEM (n = 8). **P* < 0.05 compared with the HFD group (Dunnett post hoc test).

Figure 4. Histological evaluation of epididymal adipose tissue in mice fed (A) a normal-fat diet (NFD), (B) high-fat diet (HFD), (C) HFD supplemented with *Lactobacillus curvatus* #4G2, and (D) HFD supplemented with *Lactobacillus plantarum* Shinshu N-07;

and cross-sectional area of adipocytes in epididymal adipose tissue (E). Sections from fixed epididymal adipose tissue was stained with hematoxylin-eosin. Bar in the figure indicates 100 μm. Values are expressed as means ± SEM (n = 8). *$P < 0.05$ compared with the HFD group (Dunnett post hoc test).

Figure 5. Expression levels of lipogenesis (*Acc1*, acetyl CoA carboxylase 1; *Fas*, fatty acid synthase), β-oxidation (*Acox1*, acyl-CoA oxidase 1; *Cpt1*, carnitine palmitoyltransferase 1) and *Pparg* (peroxisome proliferator-activated receptor γ) in the liver of mice fed a high-fat diet (HFD) and HFD supplemented with *Lactobacillus curvatus* #4G2 (#4G2) or *Lactobacillus plantarum* Shinshu N-07 (N07). Values are expressed as means ± SEM (n = 8). *$P < 0.05$ compared with the HFD group (Dunnett post hoc test).

Figure 6. Expression levels of lipogenesis (*Acc1*; acetyl CoA carboxylase 1, *Fas*; fatty acid synthase), β-oxidation (*Acox1*; acyl-CoA oxidase 1, *Cpt1*; carnitine palmitoyltransferase 1), *Pparg* (peroxisome proliferator-activated receptor γ) and *Ucp1* (uncoupling protein 1) in the epididymal adipose tissue of mice fed a high-fat diet (HFD) and HFD supplemented with *Lactobacillus curvatus* #4G2 (#4G2) or *Lactobacillus plantarum* Shinshu N-07 (N07). Values are expressed as means ± SEM (n = 8). *$P < 0.05$ compared with the HFD group (Dunnett post hoc test).

Figure 7. Expression levels of inflammation markers (*Tnfa*, *Il1b*) and macrophage markers (*Cd11c*, *F4/80*) in the epididymal adipose tissue of mice fed a high-fat diet (HFD) or HFD supplemented with *Lactobacillus curvatus* #4G2 (#4G2) or *Lactobacillus plantarum* Shinshu N-07 (N07). Values are expressed as means ± SEM (n = 8).

Figure 8. Alpha diversity parameters: observed operational taxonomic units (A), Faith's phylogenetic diversity (B), principal coordinate (PC) analysis based on unweighted UniFrac distances (C), and relative abundances of o_*Lactobacillales*|f_|g_ (D), f_*Lactobacillaceae*|_ (E), and f_*S24-7*|g_ (F) of intestinal microbiota of mice fed a normal-fat diet (NFD), high-fat diet (HFD), or HFD supplemented with *Lactobacillus curvatus* #4G2 (#4G2) or *Lactobacillus plantarum* Shinshu N-07 (N07). Values are expressed as means ± SEM (n = 8). Different letters above the bar mean significant

differences ($P < 0.05$, Tukey-Kramer post hoc test).

References

Altschul, S.F., Gish, W., Miller, W., Myers, E.W., and Lipman, D.J., 1990. Basic local alignment search tool. Journal of Molecular Biology 215: 403–410. https://doi.org/10.1016/S0022-2836(05)80360-2.

Begley, M., Gahan, C.G.M., and Hill, C., 2005. The interaction between bacteria and bile. FEMS Microbiology Reviews 29: 625–651.

Berthier, F., and Ehrlich, S.D., 1999. Genetic diversity within *Lactobacillus sakei* and *Lactobacillus curvatus* and design of PCR primers for its detection using randomly amplified polymorphic DNA. International Journal of Systematic Bacteriology 49: 997–1007.

Di Cagno, R., Coda, R., De Angelis, M., and Gobbetti, M., 2013. Exploitation of vegetables and fruits through lactic acid fermentation. Food Microbiology 33: 1–10.

Callahan, B.J., McMurdie, P.J., Rosen, M.J., Han, A.W., Johnson, A.J.A., and Holmes, S.P., 2016. DADA2: High-resolution sample inference from Illumina amplicon data. Nature Methods 13: 581–583.

Campbell, C.L., Yu, R., Li, F., Zhou, Q., Chen, D., Qi, C., Yin, Y., and Sun, J., 2019. Modulation of fat metabolism and gut microbiota by resveratrol on high-fat diet-induced obese mice. Diabetes, Metabolic Syndrome and Obesity: Targets and Therapy 12: 97–107.

Chen, L., Xu, Y., Chen, X., Fang, C., Zhao, L., and Chen, F., 2017. The maturing development of gut microbiota in commercial piglets during the weaning transition. Frontiers in Microbiology 8: 1–13.

Cumbie, C.B., and Hermayer, L.K., 2008. Current concepts in targeted therapies for the pathophysiology of diabetic microvascular complications. Vascular Health and Risk Management 55: 823–832.

DeSantis, T.Z., Hugenholtz, P., Larsen, N., Rojas, M., Brodie, E.L., Keller, K., Huber, T., Dalevi, D., Hu, P., and Andersen, G.L., 2006. Greengenes, a chimera-checked 16S rRNA gene database and workbench compatible with ARB. Applied and

Environmental Microbiology 72: 5069–72. https://doi.org/10.1128/AEM.03006-05.

Fuller R., 1989. Probiotics in man and animals. Journal of Applied Bacteriology 66: 365–378.

Fusco, V., Quero, G.M., Chieffi, D., and Franz, C.M.A.P., 2016. Identification of *Lactobacillus brevis* using a species-specific AFLP-derived marker. International Journal of Food Microbiology 232: 90–94.

Guo, L.D., Yang, L.J., and Huo, G.C., 2011. Cholesterol removal by *Lactobacillus plantarum* isolated from homemade fermented cream in inner Mongolia of China. Czech Journal of Food Sciences 29: 219–225.

Hamilton, M.K., Ronveaux, C.C., Rust, B.M., Newman, J.W., Hawley, M., Barile, D., Mills, D.A., and Raybould, H.E., 2017. Prebiotic milk oligosaccharides prevent development of obese phenotype, impairment of gut permeability, and microbial dysbiosis in high fat-fed mice. American Journal of Physiology - Gastrointestinal and Liver Physiology 312: G474–G487. https://doi.org/10.1152/ajpgi.00427.2016.

Huang, Y., Wang, X., Wang, J., Wu, F., Sui, Y., Yang, L., and Wang, Z., 2013. *Lactobacillus plantarum* strains as potential probiotic cultures with cholesterol-lowering activity. Journal of dairy science 96: 2746–53. https://doi.org/10.3168/jds.2012-6123.

Joyce, S.A., MacSharry, J., Casey, P.G., Kinsella, M., Murphy, E.F., Shanahan, F., Hill, C., and Gahan, C.G.M., 2014. Regulation of host weight gain and lipid metabolism by bacterial bile acid modification in the gut. Proceedings of the National Academy of Sciences 111: 7421–7426. https://doi.org/10.1073/pnas.1323599111.

Karnik, A.A., Fields, A. V, and Shannon, R.P., 2007. Diabetic cardiomyopathy. Current Hypertension Reports 9: 467–73.

Kennedy, R., Lappin, D.F., Dixon, P.M., Buijs, M.J., Zaura, E., Crielaard, W., O'Donnell, L., Bennett, D., Brandt, B.W., and Riggio, M.P., 2016. The microbiome associated with equine periodontitis and oral health. Veterinary Research 47: 49. https://doi.org/10.1186/s13567-016-0333-1.

Kim, D.-H., Jeong, D., Kang, I.-B., Kim, H., Song, K.-Y., and Seo, K.-H., 2017. Dual function of *Lactobacillus kefiri* DH5 in preventing high-fat-diet-induced obesity: direct reduction of cholesterol and upregulation of PPAR-α in adipose tissue. Molecular Nutrition & Food Research: 1700252.

https://doi.org/10.1002/mnfr.201700252.

Klindworth, A., Pruesse, E., Schweer, T., Peplies, J., Quast, C., Horn, M., and Glöckner, F.O., 2013. Evaluation of general 16S ribosomal RNA gene PCR primers for classical and next-generation sequencing-based diversity studies. Nucleic Acids Research 41: 1–11.

Konopka, A., 2009. What is microbial community ecology. ISME Journal 3: 1223–1230.

Lee, C.J., Sears, C.L., and Maruthur, N., 2019. Gut microbiome and its role in obesity and insulin resistance. Annals of the New York Academy of Sciences: 1–16. https://doi.org/ 10.1111/nyas.14107.

Liao, C.-C., Ou, T.-T., Wu, C.-H., and Wang, C.-J., 2013. Prevention of diet-induced hyperlipidemia and obesity by caffeic acid in C57BL/6 mice through regulation of hepatic lipogenesis gene expression. Journal of Agricultural and Food Chemistry 61: 11082–11088. https://doi.org/10.1021/jf4026647.

Lim, S.-M., Jeong, J.-J., Woo, K.H., Han, M.J., and Kim, D.-H., 2016. *Lactobacillus sakei* OK67 ameliorates high-fat diet-induced blood glucose intolerance and obesity in mice by inhibiting gut microbiota lipopolysaccharide production and inducing colon tight junction protein expression. Nutrition research 36: 337–48. https://doi.org/10.1016/j.nutres.2015.12.001.

Liong, M.T., and Shah, N.P., 2005. Acid and bile tolerance and cholesterol removal ability of lactobacilli strains. Journal of Dairy Science 88: 55–66. https://doi.org/10.3168/jds.S0022-0302(05)72662-X.

Madani, G., Mirlohi, M., Yahay, M., and Hassanzadeh, A., 2013. How much *in vitro* cholesterol reducing activity of lactobacilli predicts their *in vivo* cholesterol function? International journal of preventive medicine 4: 404–13.

Masood, M.I., Qadir, M.I., Shirazi, J.H., and Khan, I.U., 2011. Beneficial effects of lactic acid bacteria on human beings. Critical Reviews in Microbiology 37: 91–98. https://doi.org/10.3109/1040841X.2010.536522.

McDonald, D., Price, M.N., Goodrich, J., Nawrocki, E.P., Desantis, T.Z., Probst, A., Andersen, G.L., Knight, R., and Hugenholtz, P., 2012. An improved Greengenes taxonomy with explicit ranks for ecological and evolutionary analyses of bacteria and archaea. ISME Journal 6: 610–618. https://doi.org/10.1038/ismej.2011.139.

Million, M., Angelakis, E., Paul, M., Armougom, F., Leibovici, L., and Raoult, D.,

2012. Comparative meta-analysis of the effect of *Lactobacillus* species on weight gain in humans and animals. Microbial Pathogenesis 53: 100–108. https://doi.org/10.1016/j.micpath.2012.05.007.

Miyoshi, M., Ogawa, A., Higurashi, S., and Kadooka, Y., 2014. Anti-obesity effect of *Lactobacillus gasseri* SBT2055 accompanied by inhibition of pro-inflammatory gene expression in the visceral adipose tissue in diet-induced obese mice. European Journal of Nutrition 53: 599–606.

Ogita, T., Tanii, Y., Morita, H., and Tanabe, S., 2011. Suppression of Th17 response by *Streptococcus thermophilus* ST28 through induction of IFN-γ. International Journal of Molecular Medicine 28: 817–822. https://doi.org/10.3892/ijmm.2011.755.

Olefsky, J.M., and Glass, C.K., 2010. Macrophages, Inflammation, and Insulin Resistance. Expert Opinion on Therapeutic Targets 19: 1-28. https://doi.org/ 10.1146/annurev-physiol-021909-135846.

Orci, L., Cook, W.S., Ravazzola, M., Wang, M., Park, B.-H., Montesano, R., and Unger, R.H., 2004. Rapid transformation of white adipocytes into fat-oxidizing machines. Proceedings of the National Academy of Sciences 101: 2058–2063. https://doi.org/10.1073/pnas.0308258100.

Ormerod, K.L., Wood, D.L.A., Lachner, N., Gellatly, S.L., Daly, J.N., Parsons, J.D., Dal'Molin, C.G.O., Palfreyman, R.W., Nielsen, L.K., Cooper, M.A., Morrison, M., Hansbro, P.M., and Hugenholtz, P., 2016. Genomic characterization of the uncultured Bacteroidales family S24-7 inhabiting the guts of homeothermic animals. Microbiome 4: 1–17.

Park, S., Ji, Y., Jung, H.-Y., Park, H., Kang, J., Choi, S.-H., Shin, H., Hyun, C.-K., Kim, K.-T., and Holzapfel, W.H., 2017. *Lactobacillus plantarum* HAC01 regulates gut microbiota and adipose tissue accumulation in a diet-induced obesity murine model. Applied Microbiology and Biotechnology 101: 1605–1614. https://doi.org/10.1007/s00253-016-7953-2.

Parvez, S., Malik, K.A., Ah Kang, S., and Kim, H.Y., 2006. Probiotics and their fermented food products are beneficial for health. Journal of Applied Microbiology 100: 1171–1185.

Reeves, P.G., Nielsen, F.H., and Fahey, G.C., 1993. AIN-93 purified diets for laboratory rodents: final report of the American Institute of Nutrition ad hoc

writing committee on the reformulation of the AIN-76A rodent diet. The Journal of Nutrition 123: 1939–51.

Russo, L., and Lumeng, C.N., 2018. Properties and functions of adipose tissue macrophages in obesity. Immunology 155: 407–417.

Sandagdorj, B., Hamajima, C., Kawahara, T., Watanabe, J., and Tanaka, S., 2019. Characterization of microbiota that influence immunomodulatory effects of fermented *Brassica rapa* L. Microbes and Environments 34: 206–214. https://doi.org/10.1264/jsme2.ME19003.

Sanz, Y., Santacruz, A., and Gauffin, P., 2010. Gut microbiota, obesity and metabolic disorders. Proceedings of the Nutrition Socoety 69: 434–441.

Segata, N., Izard, J., Waldron, L., Gevers, D., Miropolsky, L., Garrett, W.S., and Huttenhower, C., 2011. Metagenomic biomarker discovery and explanation. Genome Biology 12: R60. https://doi.org/ 10.1186/gb-2011-12-6-r60.

Serino, M., Luche, E., Gres, S., Baylac, A., Bergé, M., Cenac, C., Waget, A., Klopp, P., Iacovoni, J., Klopp, C., Mariette, J., Bouchez, O., Lluch, J., Ouarné, F., Monsan, P., Valet, P., Roques, C., Amar, J., Bouloumié, A., et al., 2012. Metabolic adaptation to a high-fat diet is associated with a change in the gut microbiota. Gut 61: 543–553.

De Smet, I., De Boever, P., and Verstraete, W., 1998. Cholesterol lowering in pigs through enhanced bacterial bile salt hydrolase activity. The British Journal of Nutrition 79: 185–94. https://doi.org/10.1079/bjn19980030.

Taguchi, H., Senoura, T., Hamada, S., Matsui, H., Kobayashi, Y., Watanabe, J., Wasaki, J., and Ito, S., 2008. Cloning and sequencing of the gene for cellobiose 2-epimerase from a ruminal strain of Eubacterium cellulosolvens. FEMS Microbiology Letters 287: 34–40. https://doi.org/10.1111/j.1574-6968.2008.01281.x.

Tanaka, S., Yamamoto, K., Yamada, K., Furuya, K., and Uyeno, Y., 2016. Relationship of enhanced butyrate production by colonic butyrate-producing bacteria and immunomodulatory effects in normal mice fed insoluble fraction of *Brassica rapa* L. Applied and Environmental Microbiology 82: 2693-2699. https://doi.org/10.1128/AEM.03343-15.

Tomaro-Duchesneau, C., Jones, M.L., Shah, D., Jain, P., Saha, S., and Prakash, S., 2014. Cholesterol assimilation by *Lactobacillus* probiotic bacteria: an *in vitro*

investigation. BioMed Research International 2014: 380316. https://doi.org/10.1155/2014/380316.

Tomaro-Duchesneau, C., Saha, S., Malhotra, M., Jones, M.L., Rodes, L., and Prakash, S., 2015. *Lactobacillus fermentum* NCIMB 5221 and NCIMB 2797 as cholesterol-lowering probiotic biotherapeutics: *In vitro* analysis. Beneficial Microbes 6: 861–869.

Torriani, S., Felis, E.G., and Dellaglio, F., 2001. Differentiation of *Lactobacillus plantarum*, *L. pentosus*, and *L. paraplantarum* by recA gene sequence analysis and multiplex PCR assay with recA gene-derived primers. Applied and Environmental Microbiology 67: 3450–3454.

Verwaerde, C., Delanoye, A., Macia, L., Tailleux, A., and Wolowczuk, I., 2006. Influence of high-fat feeding on both naive and antigen-experienced T-cell immune response in DO10.11 mice. Scandinavian Journal of Immunology 64: 457–466.

Wagner, M., Samdal Steinskog, E.S., and Wiig, H., 2015. Adipose tissue macrophages: the inflammatory link between obesity and cancer? Expert Opinion on Therapeutic Targets 19: 527–538.

Wolowczuk, I., Verwaerde, C., Viltart, O., Delanoye, A., Delacre, M., Pot, B., and Grangette, C., 2008. Feeding our immune system: Impact on metabolism. Clinical and Developmental Immunology 2008: 639803. https://doi.org/ 10.1155/2008/639803.

Wouters, D., Grosu-Tudor, S., Zamfir, M., and De Vuyst, L., 2013. Bacterial community dynamics, lactic acid bacteria species diversity and metabolite kinetics of traditional Romanian vegetable fermentations. Journal of the Science of Food and Agriculture 93: 749–760.

Wu, C.-C., Weng, W.-L., Lai, W.-L., Tsai, H.-P., Liu, W.-H., Lee, M.-H., Tsai, Y.-C., Wu, C.-C., Weng, W.-L., Lai, W.-L., Tsai, H.-P., Liu, W.-H., Lee, M.-H., and Tsai, Y.-C., 2015. Effect of *Lactobacillus plantarum* strain K21 on high-fat diet-fed obese mice. Evidence-Based Complementary and Alternative Medicine 2015, 2015: e391767.

Yamamoto, K., Furuya, K., Yamada, K., Takahashi, F., Hamajima, C., and Tanaka, S., 2018. Enhancement of natural killer activity and IFN-γ production in an IL-12-dependent manner by a *Brassica rapa* L. Bioscience, Biotechnology, and

Biochemistry 82: 654–668. https://doi.org/10.1080/09168451.2017.1408396.

Zhao, L., Zhang, Q., Ma, W., Tian, F., Shen, H., and Zhou, M., 2017. A combination of quercetin and resveratrol reduces obesity in high-fat diet-fed rats by modulation of gut microbiota. Food and Function 8: 4644–4656.

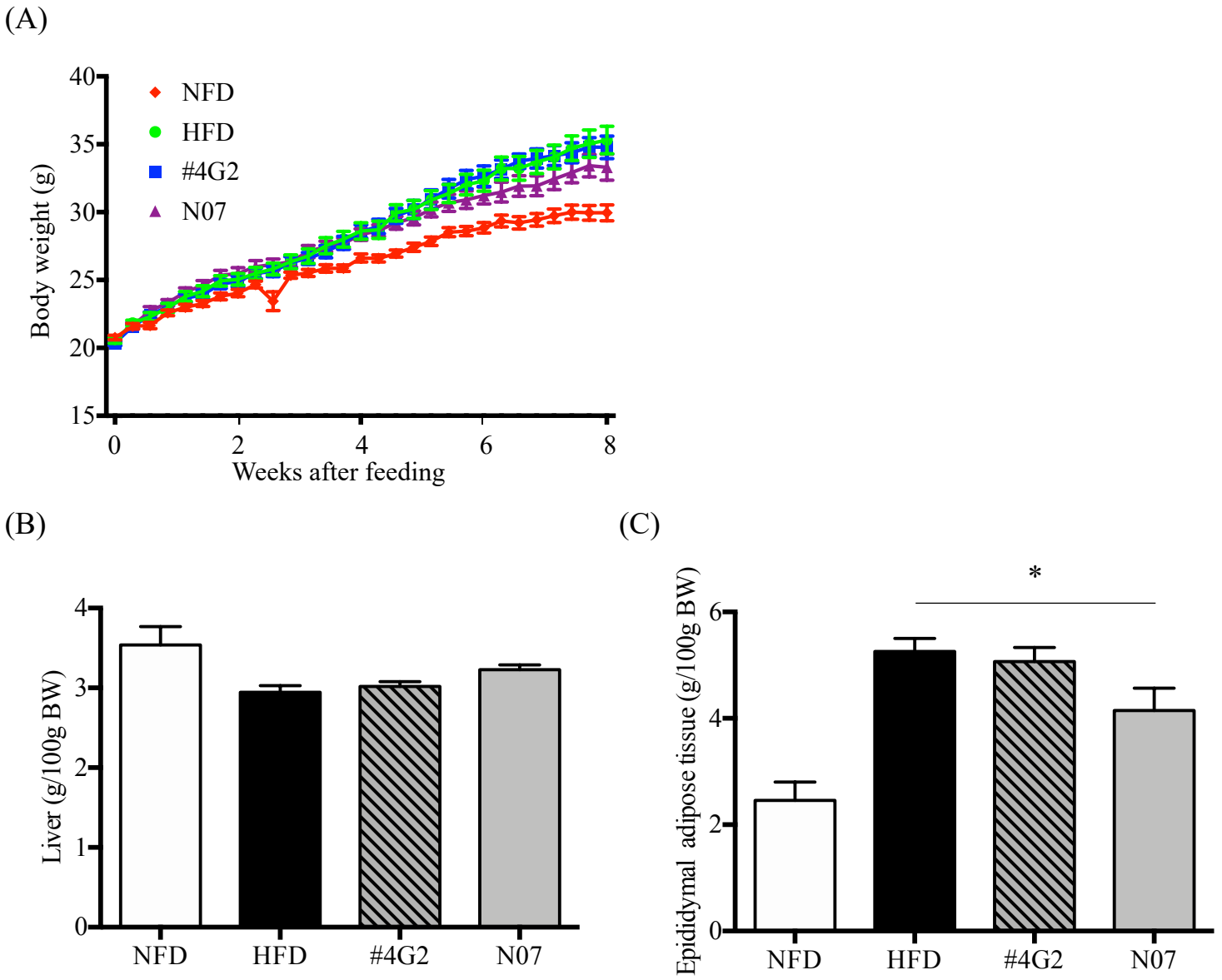
(A)
Body weight (g)
40
35
30
25
20
15
0
2
4
6
8
Weeks after feeding
NFD
HFD
#4G2
N07
(B)
Liver (g/100g BW)
4
3
2
1
0
NFD
HFD
#4G2
N07
(C)
Epididymal adipose tissue (g/100g BW)
*
6
4
2
0
NFD
HFD
#4G2
N07

Figure 1

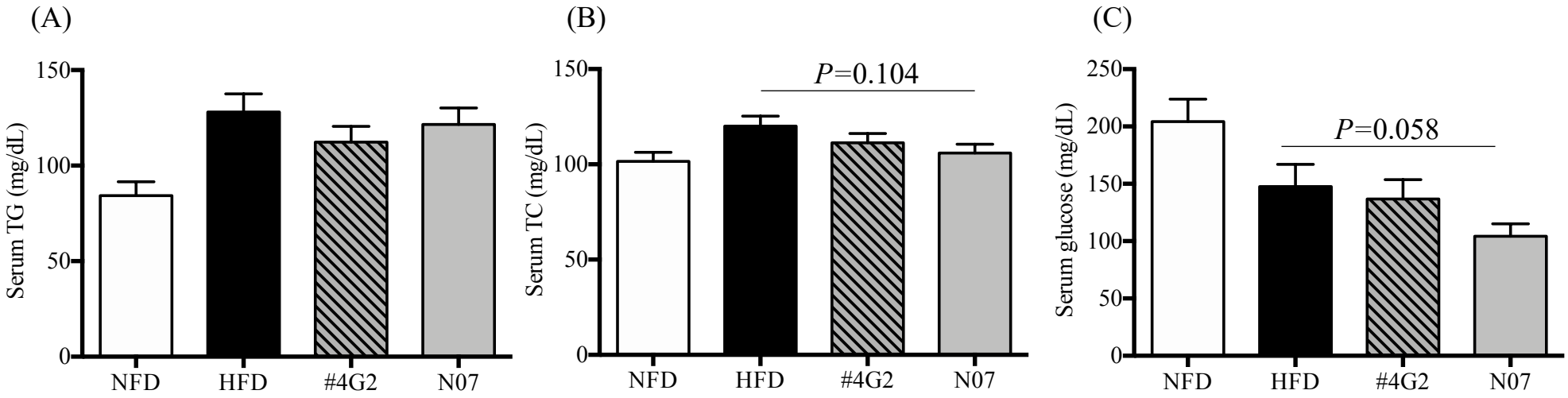
(A)
Serum TG (mg/dL)
150
100
50
0
NFD
HFD
#4G2
N07
(B)
Serum TC (mg/dL)
P=0.104
(C)
Serum glucose (mg/dL)
250
200
150
P=0.058

Figure 2

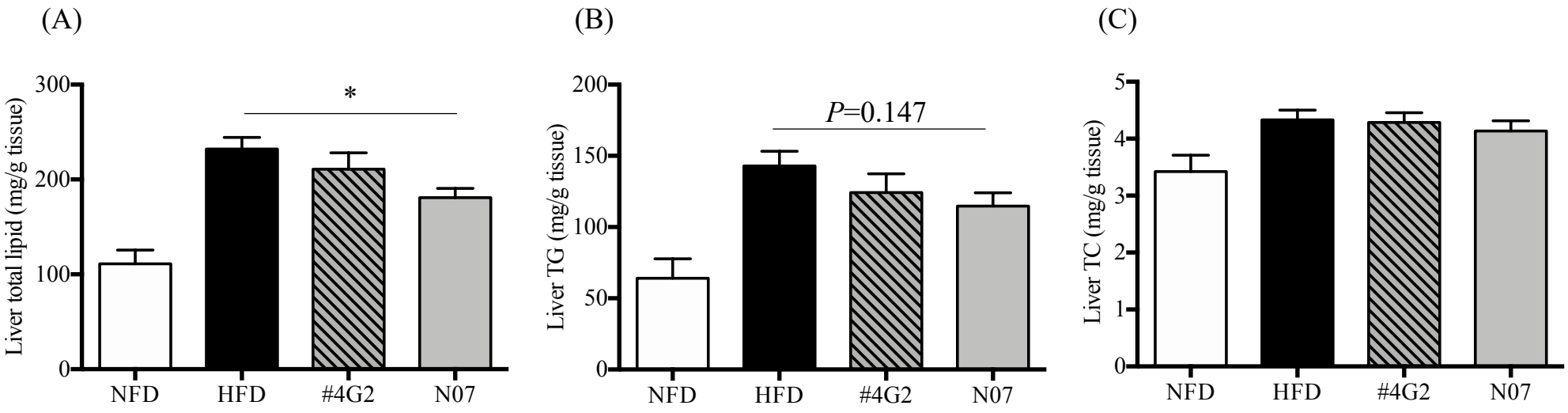
(A)
Liver total lipid (mg/g tissue)
300
200
100
0
*
NFD
HFD
#4G2
N07
(B)
Liver TG (mg/g tissue)
200
150
100
50
0
P=0.147
NFD
HFD
#4G2
N07
(C)
Liver TC (mg/g tissue)
5
4
3
2
1
0
NFD
HFD
#4G2
N07

Figure 3

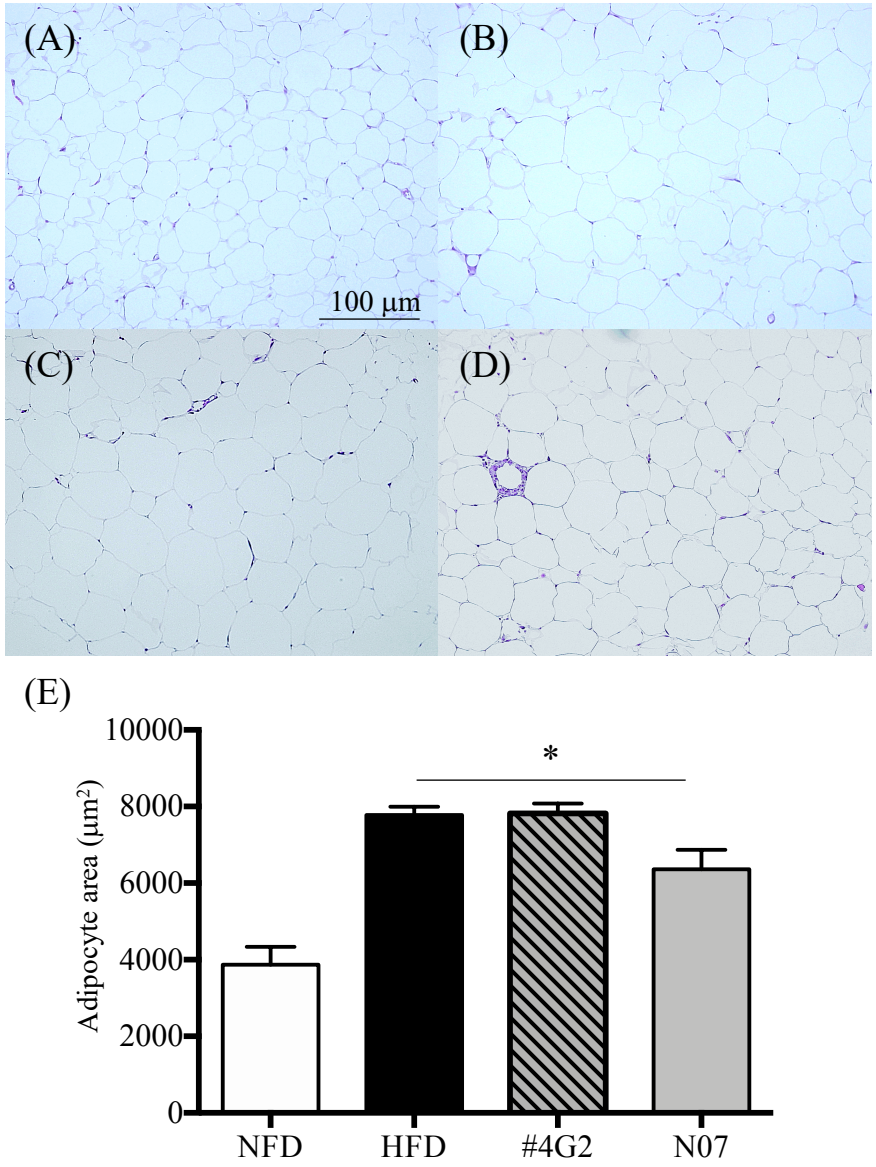
(A)
(B)
100 μm
(C)
(D)
(E)
10000
8000
6000
4000
2000
0
Adipocyte area (μm²)
*
NFD
HFD
#4G2
N07

Figure 4

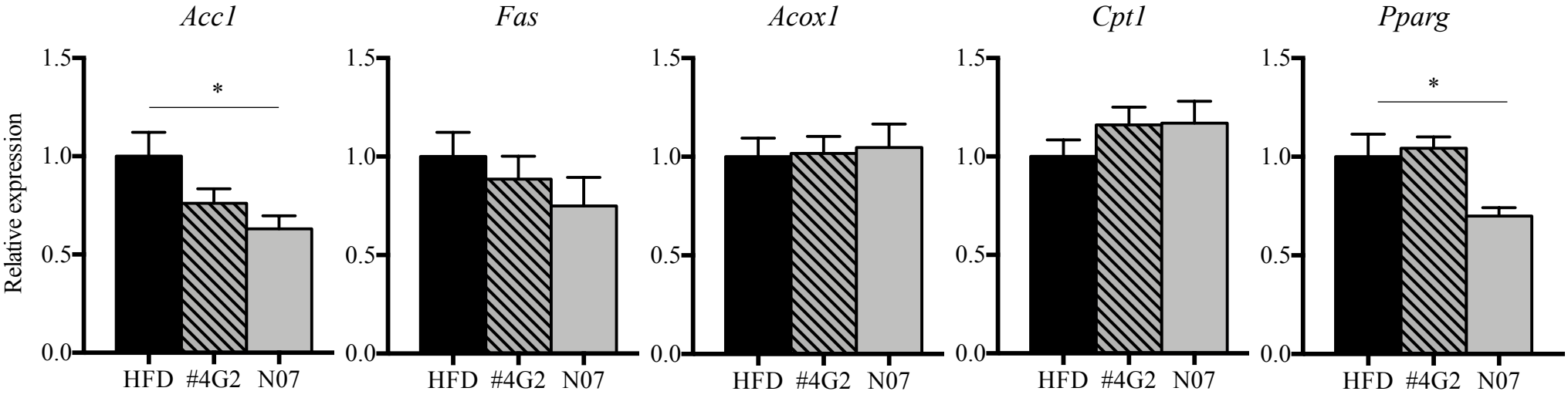
Acc1
Fas
Acox1
Cpt1
Pparg
Relative expression
1.5
1.0
0.5
0.0
*
*
HFD
#4G2
N07

Figure 5

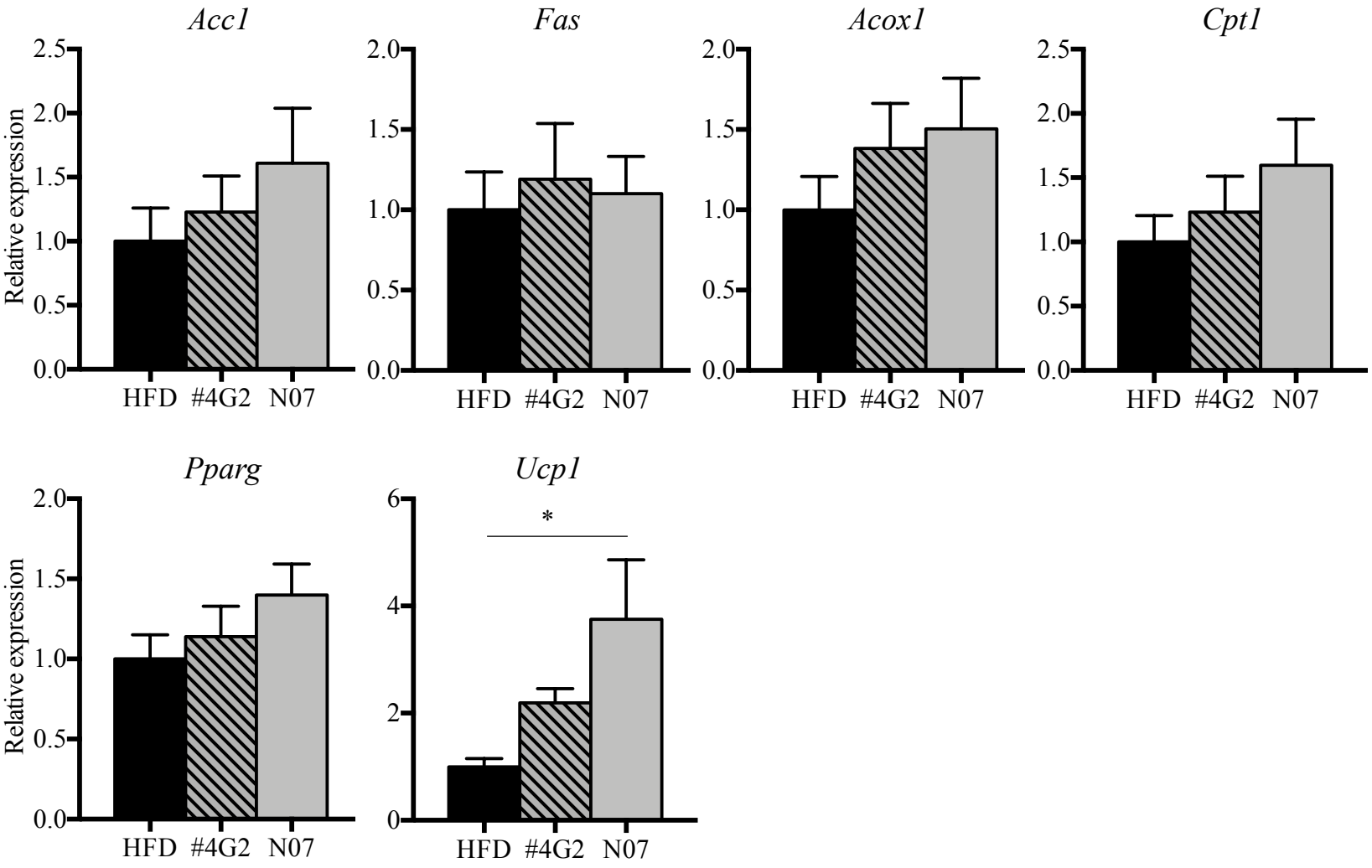
Acc1
Fas
Acox1
Cpt1
Pparg
Ucp1
Relative expression
HFD
#4G2
N07
*

Figure 6

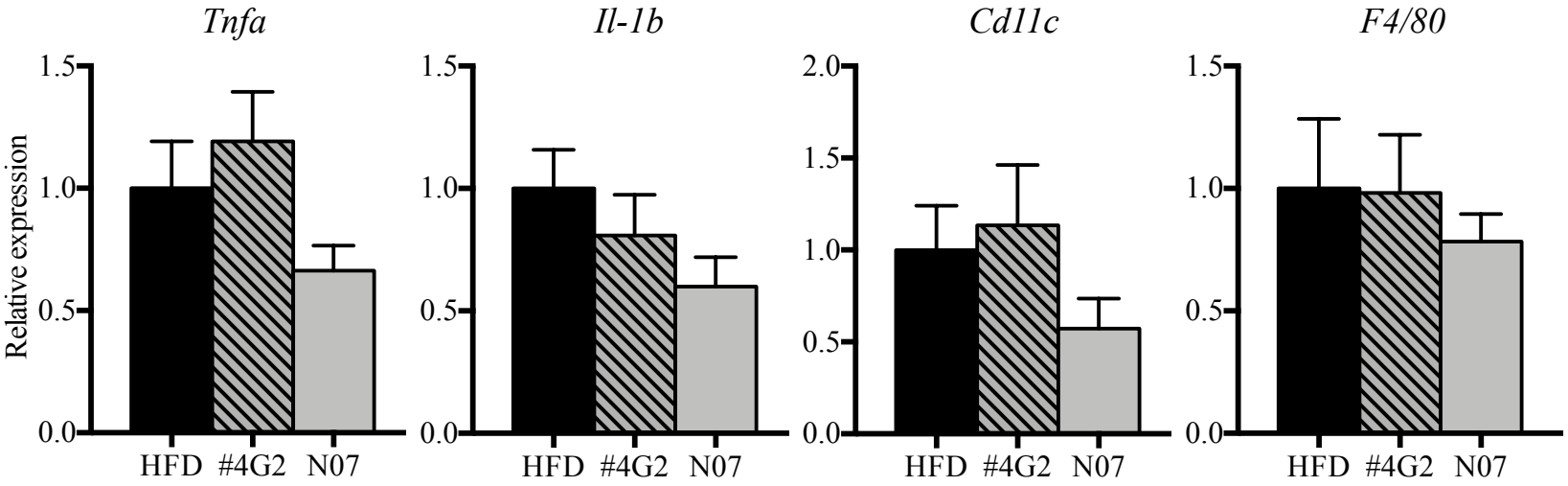
Tnfa
Il-1b
Cd11c
F4/80
Relative expression
1.5
1.0
0.5
0.0
2.0
1.5
HFD
#4G2
N07

Figure 7

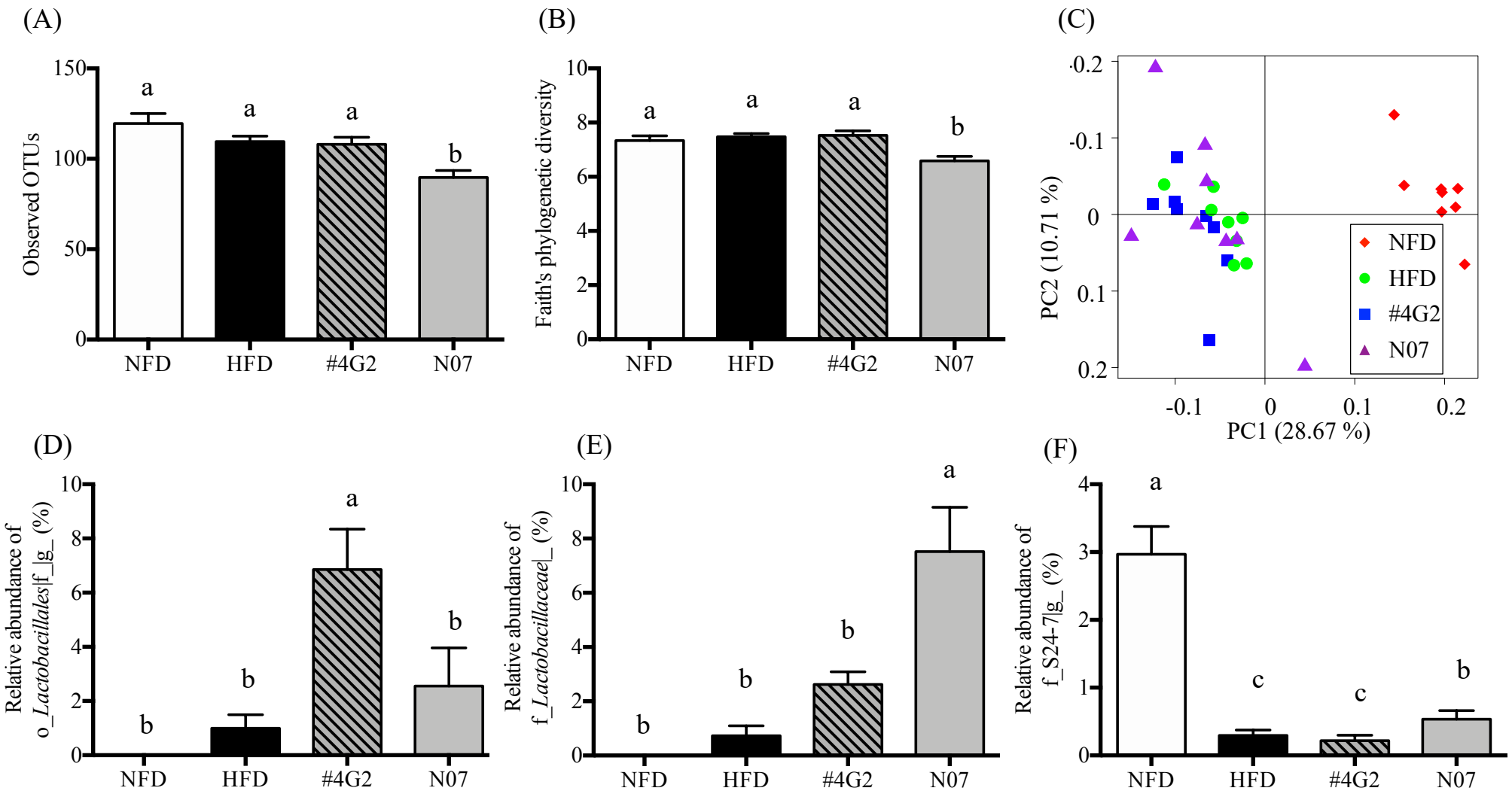
(A)
Observed OTUs
150
100
50
0
a
a
a
b
NFD
HFD
#4G2
N07
(B)
Faith's phylogenetic diversity
10
8
6
4
2
0
a
a
a
b
NFD
HFD
#4G2
N07
(C)
PC2 (10.71 %)
0.2
-0.1
0
0.1
0.2
-0.1
0
0.1
0.2
PC1 (28.67 %)
NFD
HFD
#4G2
N07
(D)
Relative abundance of o_Lactobacillales|f_|g_ (%)
10
8
6
4
2
0
b
b
a
b
NFD
HFD
#4G2
N07
(E)
Relative abundance of f_Lactobacillaceae|_ (%)
10
8
6
4
2
0
b
b
b
a
NFD
HFD
#4G2
N07
(F)
Relative abundance of f_S24-7|g_ (%)
4
3
2
1
0
a
c
c
b
NFD
HFD
#4G2
N07

Figure 8

Table S1. Primer sequences for *Lactobacillus* species-specific PCR.

Target species	Forward (5′ → 3′)	Reverse (5′ → 3′)
L. brevis	AATTGATTTTCATACCGCAGAA	TTGGCACCGCATGATGTG
L. curvatus	GCTGGATCACCTCCTTTC	TTGGTACTATTTAATTCTTAG
L. plantarum	CCGTTTATGCGGAACACCTA	TCGGGATTACCAAACATCAC

Table S2. Primer sequences for reverse transcription-PCR.

Target gene	Forward (5′ → 3′)	Reverse (5′ → 3′)
Acc1	TGTTGAGACGCTGGTTTGTAGAA	GGTCCTTATTATTGTCCCAGACGTA
Fas	GATCCTGGAACGAGAACACGA	GAGACGTGTCACTCCTGGACTTG
Acox1	CTATGGGATCAGCCAGAAAGG	AGTCAAAGGCATCCACCAAAG
Cpt1	AGACCGTGAGGAACTCAAACCTAT	TGAAGAGTCGCTCCCACT
Pparg	TGACAGGAAAGACAACAGACAAAT	GGGTGATGTGTTTGAACTTGATT
Ucp1	TGCCACACCTCCAGTCATTA	TTGGAGCTGGCTTCTGTGC
Tnfa	TGGGAGTAGACAAGGTACAACCC	CATCTTCTCAAAATTCGAGTGACAA
Il1b	GTGGACCTTCCAGGATGAGG	CGGAGCCTGTAGTGCAGTTG
Cd11c	TGTGACGGTGTCTAATGATGG	AGTTGATGCTGACTGGCACG
F4/80	CCCCAGTGTCCTTACAGAGTG	GTGCCCAGAGTGGATGTCT
Rps18	CAGTGGTCTTGGTGTGCTGA	ACCTGGAGAGGCTGAAGAAA

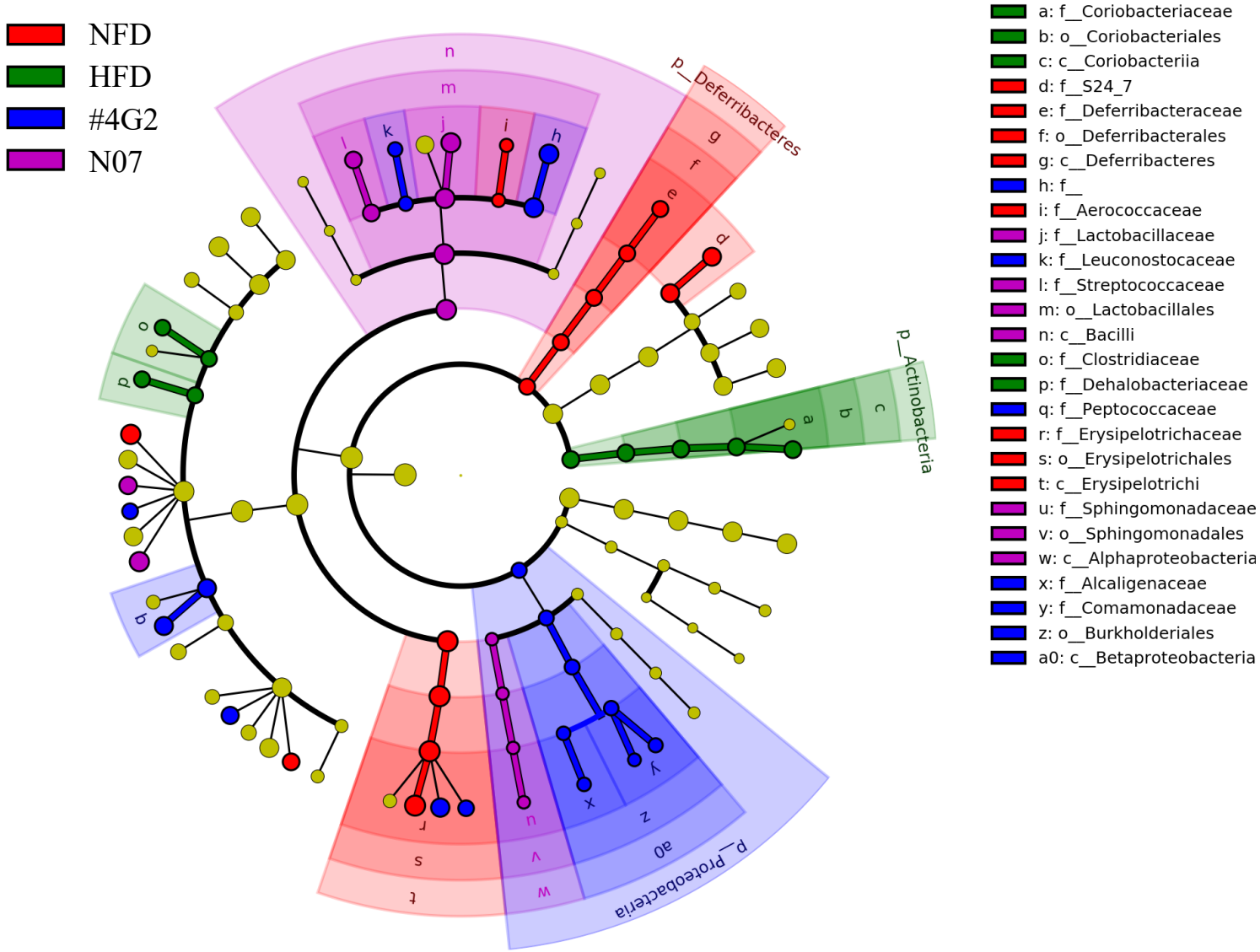

Figure S1. Cladogram for differentially abundant gut microbiota of mice fed a normal-fat diet (NFD), high-fat diet (HFD), HFD supplemented with *Lactobacillus curvatus* #4G2 (#4G2), and HFD supplemented with *Lactobacillus plantarum* Shinshu N-07 (N07) were constructed based on LEfSe analysis. Only taxa meeting an LDA significant threshold >3 are shown.